Journal of the Ceramic Society of Japan 119 [11] 894-897 2011 Note

Enhanced oxygen intake/release kinetics of $BaYMn_2O_{5+\delta}$ fine powders prepared by a wet-chemical route

Teruki MOTOHASHI,† Taku UEDA, Yuji MASUBUCHI and Shinichi KIKKAWA

Faculty of Engineering, Hokkaido University, Sapporo 060–8628

The effect of grain size on the oxygen intake/release kinetics were investigated for double-perovskite type $BaYMn_2O_{5+\delta}$ ($\delta = 0.0$–1.0). The preparation of $BaYMn_2O_{5+\delta}$ with larger specific surface area was achieved by low-temperature firing (down to 900°C) of precursors obtained from a wet-chemical route. The oxygen intake/release rates at 500°C were found to increase significantly in the resultant $BaYMn_2O_{5+\delta}$ fine powders, indicating a key role of the powder surface in the oxygen intake/release processes.

Key-words : Oxygen storage materials, Double-perovskite manganese oxides, Oxygen intake/release, Wet-chemical synthesis route

[Received June 30, 2011; Accepted August 29, 2011]

1. Introduction

Non-stoichiometric oxides which store/release oxygen reversibly at moderate temperatures are called "oxygen-storage materials (=OSMs)". OSMs have attracted increased interest for their wide applicability to oxygen-related technologies, contributing to energy generations and environmental protection.[1)–6)] The CeO_2–ZrO_2 solid solution, the so-called CZ, is the best known OSM that has been practically used as a three-way catalyst for the effective removal of NO_x, CO, and hydrocarbons from automobile exhausts.[1)] Meanwhile, a new class of OSMs is highly desirable to realize various high-temperature applications such as oxygen separation and oxidizing agents.

As promising high-performance OSMs, transition-metal oxides are worthy of attention, because of variable valence states of constituent transition metals. Recently, we found that the manganese oxide $BaYMn_2O_{5+\delta}$ shows remarkable oxygen intake/release capability at temperatures below 500°C, making this compound a strong candidate for the use in oxygen-storage applications.[6)] This oxide is categorized as an *A*-site ordered double-perovskite which contains an arrangement of smaller yttrium and larger barium ions in separate layers at the perovskite *A*-site.[6),7)] The oxygen site within the yttrium plane is readily filled/unfilled in response to the variations in temperature and/or surrounding atmosphere, leading to large oxygen non-stoichiometry ranging from $\delta = 0.0$ to 1.0.[8),9)] Note that the oxygen-storage capacity (OSC; the amount of mobile oxygen stored in the crystal lattice) of $BaYMn_2O_{5+\delta}$ reaches 3.85 wt %, being much higher than the theoretically expected value for CZ, 2.8 wt %.

$BaYMn_2O_{5+\delta}$ was originally synthesized in 1996,[7)] and has been investigated mainly from the viewpoint of solid-state physics.[10)] In the previous studies, the samples were prepared by solid-state reaction routes at temperatures above 1100°C. Such high-temperature procedures inevitably resulted in a significant grain growth. Keeping in mind that oxygen intake/release processes involve redox reactions at the powder surface and oxygen diffusion in crystallites, the control of surface area should be of particular importance. Nevertheless, no efforts were made to reduce the grain size of the $BaYMn_2O_{5+\delta}$ powder, since the oxygen storage capability of $BaYMn_2O_{5+\delta}$ had never been discussed prior to our study.

In this contribution, the oxygen intake/release kinetics of $BaYMn_2O_{5+\delta}$ fine powders is demonstrated. The preparation of $BaYMn_2O_{5+\delta}$ powders with smaller grains was achieved by low-temperature firing (down to 900°C) of precursors obtained from a wet-chemical route. The oxygen intake/release rates were found to increase significantly as the specific surface area of the sample increases, indicating a key role of the powder surface in the oxygen intake/release processes.

2. Experimental

Powder samples of $BaYMn_2O_{5+\delta}$ were synthesized via a wet-chemical route with EDTA (ethylenediaminetetraacetic acid) as a complex agent. $Ba(NO_3)_2$ (Kanto Chemical, 99%), Y_2O_3 (Wako Chemical, 99.9%; fired at 1000°C overnight prior to use), and Mn_2O_3 (Soekawa Chemical, 99.9%) were used as starting materials. A stoichiometric amount of these powders were dissolved in a concentrated HNO_3 solution in which the EDTA/NH_3 solution was subsequently added. The molar ratio of EDTA/metal ions was 1.5/1.0, as in the synthesis of hexagonal $YbMnO_3$.[11)] The EDTA complex solution was dried and combusted into a porous solid residue. This solid was ground, pelletized, and then fired at 800, 900, and 1000°C in flowing N_2 gas for 12 h. Hereafter, these samples are called "EDTA-800", "EDTA-900", and "EDTA-1000". A reference sample of $BaYMn_2O_{5+\delta}$ was also synthesized via a solid-state reaction route at 1100°C utilizing the oxygen-pressure-controlled encapsulation technique (named "SSR-1100"). Details in the solid-state reaction synthesis of $BaYMn_2O_{5+\delta}$ have been described elsewhere.[6),9)]

Phase purity and lattice parameters were checked for the resultant products by means of X-ray powder diffraction (XRD; Rigaku Ultima IV; Cu Kα radiation). The grain morphology was observed with a scanning electron microscope (SEM; JEOL JSM-6300F). The Brunauer–Emmett–Teller (BET) specific surface area of the samples was determined from N_2 adsorp-

† Corresponding author: T. Motohashi; E-mail: t-mot@eng.hokudai.ac.jp

tion isotherms measured at 77 K (Quantachrome Instruments Autosorb 6AG). The oxygen intake/release characteristics of the samples were investigated by means of thermogravimetry (TG; Rigaku TG8120GH). Approximately 20 mg of the sample powders were heated at 500°C, while isothermal TG data were measured upon switching the atmosphere between 5% H_2/95% Ar gas mixture and O_2.

3. Results and discussion

It has been indicated that the control of oxygen partial pressure is indispensable to obtain $BaYMn_2O_{5+\delta}$. This oxide was found to be formed only in strongly reductive conditions,[7)–9)] suggesting the difficulty in phase formation at low temperatures. In the present work, lowering of the synthesis temperature was achieved using precursors prepared by the EDTA complex polymerization route. **Figure 1** shows XRD patterns for the as-synthesized products of EDTA-800, EDTA-900, EDTA-1000, and SSR-1100 (reference). The EDTA-900 and EDTA-1000 products contain double-perovskite type $BaYMn_2O_{5+\delta}$ as a main phase. Most of the diffraction peaks are readily indexed on the basis of the tetragonal $P4/nmm$ space group. The lattice parameters were calculated to be $a \approx 0.554$ nm and $c \approx 0.766$ nm, in good agreement with those of $BaYMn_2O_5$ (i.e., $\delta = 0$) in the literature.[8),9)] While SSR-1100 is essentially the single phase of $BaYMn_2O_5$, EDTA-900 and EDTA-1000 contain small amounts (~5 wt %) of $BaMnO_{3-\delta}$ and Y_2O_3 as secondary phases. EDTA-800 is a mixture of $BaMnO_{3-\delta}$ and Y_2O_3 with no trace of $BaYMn_2O_5$. The crystallite size of $BaYMn_2O_5$ was estimated with Sherrer's equation to be 110, 86, and 36 nm for SSR-1100, EDTA-1000, and EDTA-900, respectively.

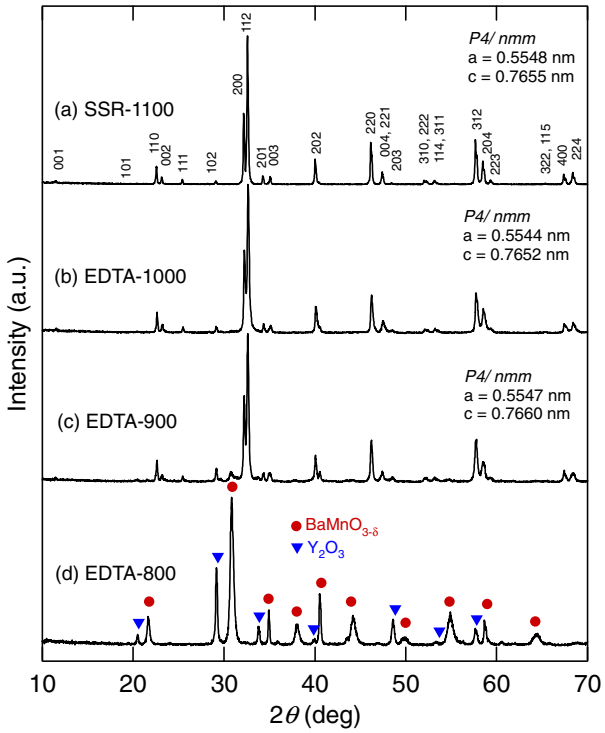

Fig. 1. (Color online) X-ray powder diffraction patterns for the $BaYMn_2O_{5+\delta}$ products. (a) SSR-1100, (b) EDTA-1000, (c) EDTA-900, and (d) EDTA-800. Diffraction peaks of $BaMnO_{3-\delta}$ and Y_2O_3 are marked with red circles and blue triangles, respectively.

It should be emphasized that the use of precursors via the EDTA route is a key factor in realizing the low-temperature synthesis of $BaYMn_2O_5$. In fact, this oxide never formed in flowing N_2 gas at $T \leq 1000$°C when starting from a solid-state mixture of $BaCO_3$, Y_2O_3, and Mn_2O_3. High degree of chemical homogeneity of the precursor is believed to facilitate the phase formation of $BaYMn_2O_5$. Meanwhile, TG analysis of the precursor revealed a significant weight loss (~40 wt %) upon heating in flowing N_2, which is attributed to combustion (oxidation) of organic residues in the precursor. Such a combustion reaction of the residues may induce a reductive atmosphere in local environment, and thereby stabilize the $BaYMn_2O_5$ phase during the heat treatment.

In **Fig. 2**, typical SEM images of EDTA-900, EDTA-1000, and SSR-1100 are presented. The SSR-1100 product contains large grains of several micrometers, indicating a significant grain growth in this product. On the other hand, the grain morphology is apparently different in EDTA-900 and EDTA-1000. These products consist of porous agglomerates of fine primary particles. The size of the primary particles, ~0.2 and ~1 μm for EDTA-900 and EDTA-1000, respectively, is much smaller than that for SSR-1100. Obviously, lowering of the synthesis temperature effectively suppresses the grain growth. The presence of organic residues in the precursor may contribute to the formation of porous microstructure in the EDTA-route products. The specific surface area (s) of the products is summarized in **Table 1**. As expected from the SEM observation, the s values are accordingly enhanced as the synthesis temperature is lowered.

To investigate the effect of powder morphology on the oxygen intake/release kinetics, isothermal TG curves were measured at 500°C upon switching the atmosphere between 5% H_2/95%

Table 1. The average grain size and specific surface area (s) of the samples

Sample name	Synthesis route	Firing temperature (°C)	Average grain size (μm)	Specific surface area s ($m^2\,g^{-1}$)
SSR-1100	Solid-state reaction	1100	~5	0.5
EDTA-1000	Wet chemistry	1000	~1	1.2
EDTA-900	Wet chemistry	900	~0.2	3.0

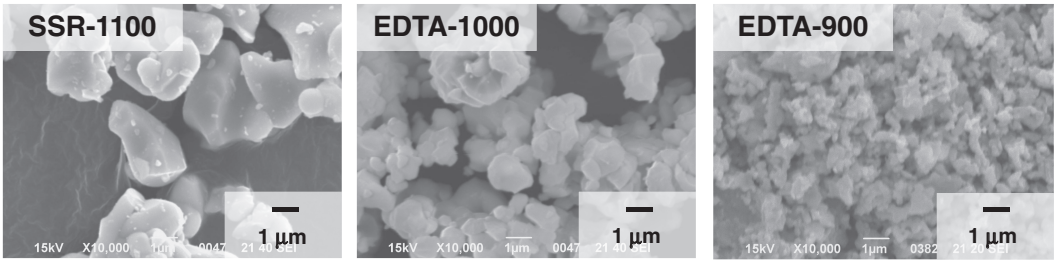

Fig. 2. SEM images of the $BaYMn_2O_{5+\delta}$ products: (left) SSR-1100, (middle) EDTA-1000, and (right) EDTA-900.

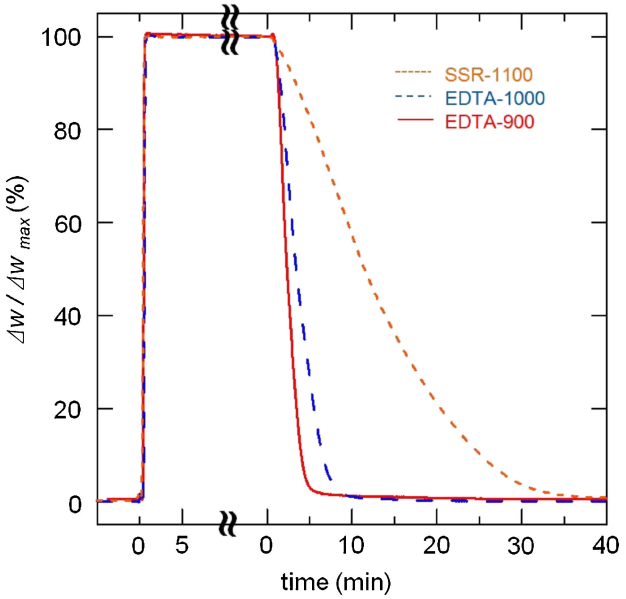

Fig. 3. (Color online) Isothermal TG curves ($\Delta w/\Delta w_{max}$ vs. time plots) for the $BaYMn_2O_{5+\delta}$ samples. The measurements were carried out at 500°C while the gas flow was switched from 5% H_2/95% Ar to O_2, and then to 5% H_2/95% Ar. The data of SSR-1100, EDTA-1000, and EDTA-900 are shown with dotted (orange), broken (blue), and solid (red) curves, respectively.

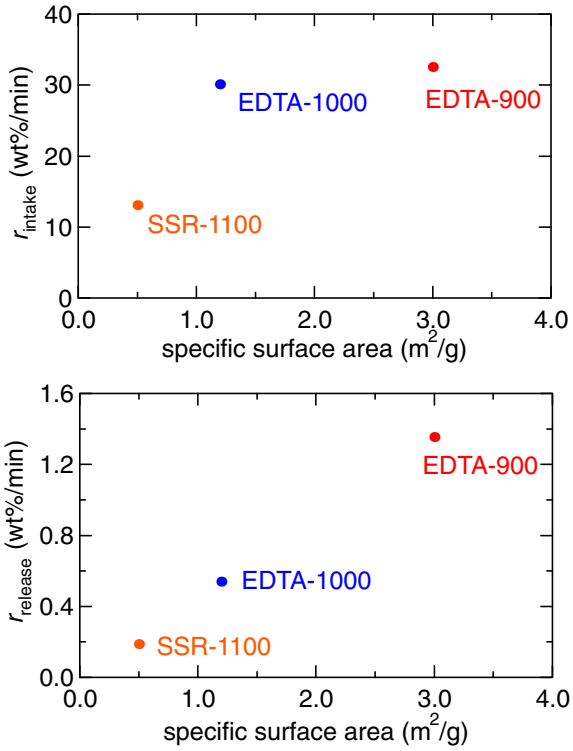

Fig. 4. (Color online) The oxygen intake and release rates, r_{intake} and $r_{release}$, of the $BaYMn_2O_{5+\delta}$ samples against the specific surface area (s) of the samples. The r_{intake} and $r_{release}$ values are defined as slopes of the $\Delta w/\Delta w_{max}$ vs. time plot at 50% of the maximum weight variation.

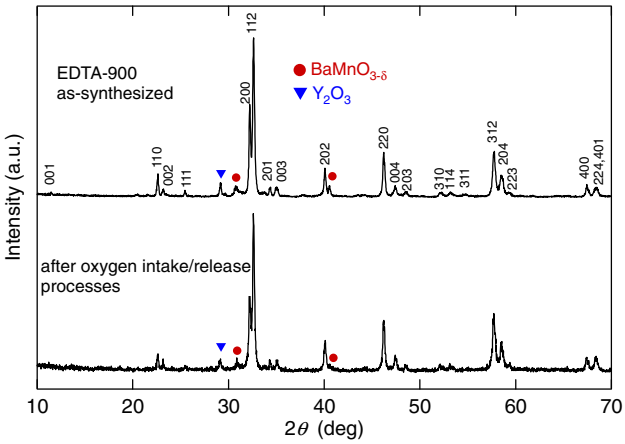

Fig. 5. (Color online) X-ray powder diffraction patterns for the EDTA-900 sample before and after the oxygen intake/release cyclic test (see main text). Diffraction peaks of $BaMnO_{3-\delta}$ and Y_2O_3 are marked with red circles and blue triangles, respectively.

Ar and O_2. For all of the EDTA-900, EDTA-1000, and SSR-1100 samples, remarkable oxygen intake/release phenomena were observed in response to the gas switching. The magnitude of weight gain/loss (=OSC) was approximately 3.7 wt %, being comparable to the ideal OSC value (3.85 wt %). In **Fig. 3**, the normalized weight variation $\Delta w/\Delta w_{max}$, where Δw_{max} is the maximum weight variation upon oxygen intake, is plotted as a function of time. While the oxygen intake process is always fast and completed only within 20 s in all the samples, the response of oxygen release significantly depends on the synthesis condition. In fact, as the specific surface area of the sample increases, the time required for complete oxygen release is effectively shortened from 40 min ($s = 0.5\,m^2\,g^{-1}$), 10 min ($1.2\,m^2\,g^{-1}$), and 5 min ($3.0\,m^2\,g^{-1}$). From the TG data, the oxygen intake/release rates, r_{intake} and $r_{release}$, are estimated and plotted as a function of the specific surface area (s) in **Fig. 4**. The r_{intake} and $r_{release}$ values are defined as slopes of the $\Delta w/\Delta w_{max}$ vs. time plot at 50% of the maximum weight variation. The r_{intake} value is an order of magnitude larger than that of $r_{release}$, and accordingly enhanced as the s value increases. The influence of powder surface area is more remarkable for the oxygen release process: $r_{release}$ is indeed proportional to the s value of the sample, leading to the drastically enhanced oxygen intake/release kinetics in the $BaYMn_2O_{5+\delta}$ fine powders.

The thermal durability of the resultant $BaYMn_2O_{5+\delta}$ fine powder was tested by repeating oxygen intake/release processes: the EDTA-900 sample was heated at 500°C while the gas flow was switched every 10 min from O_2 and 5% H_2/95% Ar and vice versa. As evidenced in **Fig. 5**, the XRD pattern for the sample after 100 cycles is essentially identical to that for the as-synthesized product, demonstrating a perfect cyclic durability of our $BaYMn_2O_{5+\delta}$ fine powder.

It can be assumed that the oxygen intake/release processes of $BaYMn_2O_{5+\delta}$ proceed with the following three steps: (1) adsorptions of reactant gas molecules (O_2 for oxygen intake; H_2 for oxygen release), (2) redox reactions at the powder surface (reduction of O_2 to form two O^{2-} ions for oxygen intake; reaction between H_2 and O^{2-} to form H_2O for oxygen release), (3) bulk diffusions of O^{2-} ions. Taking into account the experimental fact that the magnitude of r_{intake} is much larger than that of $r_{release}$, the bulk diffusion rate is likely to be fast enough at 500°C, since both the oxygen intake/release processes involve bulk diffusions. The strong correlation between the oxygen release kinetics and powder surface area (see the lower panel of Fig. 4) clearly indicates dominant roles of the surface reactions in the overall reaction rate. Meanwhile, the large r_{intake} value may be related to

a high formation rate of O^{2-} ions at the powder surface, implying a significant electron-donating ability of this oxide.

With the present experimental condition, detailed analysis on the oxygen intake/release kinetics may not be possible due to instantaneous evolutions of large exothermic/endothermic heats upon oxygen intake/release. Additional TG experiments involving moderate reaction rates at lower temperatures are necessary for deeper understanding of the oxygen intake/release mechanism of $BaYMn_2O_{5+\delta}$.

4. Conclusions

The enhanced oxygen intake/release kinetics of $BaYMn_2O_{5+\delta}$ fine powders was demonstrated. The preparation of $BaYMn_2O_{5+\delta}$ with larger specific surface area (s) was achieved by low-temperature firing (down to 900°C) of precursors obtained from a wet-chemical route with EDTA as a complex agent. While the oxygen intake process at 500°C was always fast and completed only within 20 s, the time required for complete oxygen release was effectively shortened from 40 to 5 min, as the s value of the sample was increased from 0.5 to $3.0\,m^2\,g^{-1}$. The present work clearly indicates the importance of grain size control of $BaYMn_2O_{5+\delta}$ powders. We note that $s = 3.0\,m^2\,g^{-1}$ of our product is still smaller than $s > 50\,m^2\,g^{-1}$ reported for CZ, the conventional OSM in three-way catalysts.[1)] Further efforts are thus necessary to fabricate $BaYMn_2O_{5+\delta}$ powders with smaller grains for enhancing oxygen intake/release characteristics.

Acknowledgment We are grateful to Dr. K. Oshima and Dr. T. Setoyama (Mitsubishi Chemical Group, Science and Technology Research Center, Inc.) for their discussion and comments. The present work was supported by a Grant-in-Aid for Science Research (Contract No. 22750181) from the Japan Society for the Promotion of Science. T.M acknowledges financial support from Inamori Foundation.

References

1) See e.g., J. Kašpar and P. Fornasiero, *J. Solid State Chem.*, 171, 19–29 (2003).
2) M. Machida, K. Kawamura, K. Ito and K. Ikeue, *Chem. Mater.*, 17, 1487–1492 (2005).
3) M. Karppinen, H. Yamauchi, S. Otani, T. Fujita, T. Motohashi, Y.-H. Huang, M. Valkeapää and H. Fjellvåg, *Chem. Mater.*, 18, 490–494 (2006).
4) T. Motohashi, S. Kadota, H. Fjellvåg, M. Karppinen and H. Yamauchi, *Mater. Sci. Eng., B*, 148, 196–198 (2008).
5) P. Singh, M. S. Hegde and J. Gopalakrishnan, *Chem. Mater.*, 20, 7268–7273 (2008).
6) T. Motohashi, T. Ueda, Y. Masubuchi, M. Takiguchi, T. Setoyama, K. Oshima and S. Kikkawa, *Chem. Mater.*, 22, 3192–3196 (2010).
7) J. P. Chapman, J. P. Attfield, M. Molgg, C. M. Friend and T. P. Beales, *Angew. Chem., Int. Ed. Engl.*, 35, 2482–2484 (1996).
8) F. Millange, E. Suard, V. Caignaert and B. Raveau, *Mater. Res. Bull.*, 34, 1–9 (1999).
9) M. Karppinen, H. Okamoto, H. Fjellvåg, T. Motohashi and H. Yamauchi, *J. Solid State Chem.*, 177, 2122–2128 (2004).
10) See e.g., T. Nakajima, H. Kageyama, H. Yoshizawa and Y. Ueda, *J. Phys. Soc. Jpn.*, 71, 2843–2846 (2002).
11) Y. H. Huang, H. Fjellvåg, M. Karppinen, B. C. Hauback, H. Yamauchi and J. B. Goodenough, *Chem. Mater.*, 18, 2130–2134 (2006).